JOURNAL OF BACTERIOLOGY, Mar. 1997, p. 1541–1549 Vol. 179, No. 5
0021-9193/97/$04.00+0

Catabolite Inactivation of the Galactose Transporter in the Yeast *Saccharomyces cerevisiae*: Ubiquitination, Endocytosis, and Degradation in the Vacuole

JAROSLAV HORAK[1] AND DIETER H. WOLF[2]*

Institute of Physiology, Department of Membrane Transport, Academy of Sciences of the Czech Republic, 142 20 Prague, Czech Republic,[1] and Institut für Biochemie der Universität Stuttgart, D-70569 Stuttgart, Germany[2]

Received 18 October 1996/Accepted 27 December 1996

When *Saccharomyces cerevisiae* cells growing on galactose are transferred onto glucose medium containing cycloheximide, an inhibitor of protein synthesis, a rapid reduction of Gal2p-mediated galactose uptake is observed. We show that glucose-induced inactivation of Gal2p is due to its degradation. Stabilization of Gal2p in *pra1* mutant cells devoid of vacuolar proteinase activity is observed. Subcellular fractionation and indirect immunofluorescence showed that the Gal2 transporter accumulates in the vacuole of the mutant cells, directly demonstrating that its degradation requires vacuolar proteolysis. In contrast, Gal2p degradation is proteasome independent since its half-life is unaffected in *pre1-1 pre2-2*, *cim3-1*, and *cim5-1* mutants defective in several subunits of the protease complex. In addition, vacuolar delivery of Gal2p was shown to be blocked in conditional *end3* and *end4* mutants at the nonpermissive temperature, indicating that delivery of Gal2p to the vacuole occurs via the endocytic pathway. Taken together, the results presented here demonstrate that glucose-induced proteolysis of Gal2p is dependent on endocytosis and vacuolar proteolysis and is independent of the functional proteasome. Moreover, we show that Gal2p is ubiquitinated under conditions of glucose-induced inactivation.

In the yeast *Saccharomyces cerevisiae*, galactose transport proceeds via a rather specific transporter-mediated process of facilitated diffusion. The *GAL2* gene product, which is inducible by its own substrate, is thought to be the major component of transport (11, 40). The Gal2 transporter was predicted to be a 63.7-kDa integral plasma membrane protein containing 12 putative membrane-spanning helices connected by hydrophilic charged loops (37, 53). A limited sequence of 101 amino acid residues that consists of membrane-spanning segments 10 to 12 and about 18 amino acids of the hydrophilic carboxy terminus was shown to be important for substrate recognition (38). Gal2p belongs to a superfamily of sugar transporters of prokaryotes and eukaryotes, sharing high similarity and several motifs of potential structural and/or functional importance (4). An analysis of Gal2p in temperature-conditional *sec* mutants showed that its delivery to the cell surface requires a functional secretory pathway (55). In contrast to the inducibility of Gal2p by galactose, glucose as a readily fermentable carbon source was shown to negatively influence its transport activity in galactose-grown cells at two different levels. One is represented by repression of *GAL2* gene transcription, and the second occurs at the posttranslational level by a mechanism called glucose-induced inactivation or catabolite inactivation (25). Earlier experiments with galactose (11, 35), maltose (5), and unspecified high-affinity glucose (6) transport systems have revealed their inactivation to be a relatively rapid and irreversible process that requires arrest of cytosolic protein synthesis either by nitrogen source deprivation or cycloheximide addition to the medium and the presence of a readily fermentable sugar. The inactivation follows first-order kinetics and mostly results in a serious decrease in the maximum capacity of the corresponding transporters, leaving the K_m values for their substrates unchanged. All of these characteristics implied that catabolite inactivation could be due to the breakdown of the transporters.

We have raised polyclonal antibodies against the recombinant galactose transporter Gal2p to analyze its localization and the molecular mechanism of catabolite inactivation using mutants defective in two major proteolytic systems of the cell, the proteasome and the vacuole (lysosome). The predicted plasma membrane location of Gal2p was confirmed by immunofluorescence and subcellular fractionation experiments. Internalization of Gal2p was studied using mutants defective in endocytosis. We provide experimental evidence that the Gal2 transporter is a relatively short-lived protein which is delivered from the plasma membrane to the vacuole via endocytosis. Proteolytic degradation is carried out by vacuolar proteinases. Ubiquitination of the galactose transporter in response to glucose-induced inactivation was demonstrated.

MATERIALS AND METHODS

Plasmids. YEp96 is a 2μm *S. cerevisiae*-based shuttle vector that contains a synthetic gene for yeast ubiquitin (Ub) under the control of the copper-inducible *CUP1* promoter, YEp112 encodes yeast Ub with an additional epitope from the hemagglutinin (Ha) of influenza virus attached to its amino terminus (Ha-Ub). Both plasmids were a gift from M. Hochstrasser (15). pS25 is a 2μm *S. cerevisiae-Escherichia coli* vector that carries the *GAL2* gene under the control of its own promoter. pHR98 is identical to pS25, with the difference that instead of the wild-type *GAL2* it encodes a *gal2*::*HIS3* version from which *GAL2* is deleted. The plasmids were a gift from H. Ronne (37).

Strains and growth conditions. The *S. cerevisiae* strains used were wild-type WCG4α (*MAT*α *ura3 his3-11,15 leu2-3,112*) and its isogenic derivatives YMTA (*MAT*α *pra1ΔEN*::*HIS3 ura3 his3-11,15 leu2-3,112*) (47) and WCG4-11/22, carrying the *pre1-1* and *pre2-2* mutations (18, 19), and wild-type strain RH144-3D (*MAT*α *ura3 his4 leu2 bar1-1*) and its isogenic derivatives RH266-1D (*MAT*α *ura3 his4 leu2 bar1-1 end3*) and RH268-1C (*MAT*α *ura3 his4 leu2 bar1-1 end4*). The strains were gifts from H. Riezman (41). Strains CMY762 (*MAT***a** *ura3-52 leu2-Δ1 his3Δ-200 cim3-1*) and CMM806 (*MAT***a** *ura3-52 leu2-Δ1 his3Δ-200 cim5-1*) and congenic wild-type strain YPG499 (*MAT***a** *ura3-52 leu2-Δ1 his3Δ-200 trp1-Δ63 lys2-801 ade2-101*) were gifts from C. Mann (17). For overexpression of the different Ub variants, the wild-type strain W303-1B (*MAT*α *ade2-1 leu2-3,112 his3-11,15 trp1-1 ura3-1*) and its *gal2*::*HIS3* mutant derivative were transformed

* Corresponding author. Phone: 49-711-685-4390. Fax: 49-711-685-4392.

with plasmid YEp96 or YEp112, respectively. The wild-type strain was a gift from H.-L. Chiang (8).

Cell cultures were grown on mineral medium (0.67% Difco yeast nitrogen base without amino acids) containing 2% glucose, 2% raffinose, or 2 and 5% galactose as sole carbon source and appropriate supplements. Radiolabeling was performed with pulse medium (0.17% Difco yeast nitrogen base without amino acids and ammonium sulfate, 0.5% proline, 100 μM ammonium sulfate) containing 2 or 5% galactose as a carbon source and supplements.

The linearized *gal2*::*HIS3*-containing 5.7-kb fragment was obtained by *Eco*RI cleavage of pHR98 (36), electrophoretically purified, and used to transform the yeast strains WCG4 and W303-1B. Transformants with the gal2$^-$ His$^+$ phenotype were selected, and the correct disruption of the *GAL2* open reading frame was confirmed by Southern blot analysis.

Preparation of Gal2p antibody. For the production of antibody specific to the Gal2 transporter protein, an MS2 polymerase-Gal2 protein fusion was constructed with the expression vector pEx31b, which contains the 99 amino-terminal amino acid residues of MS2 polymerase under the control of the inducible λP_L promoter as described elsewhere (42). An approximately 0.5-kb *Stu*I-*Xba*I fragment of plasmid pS25, encoding amino acids 524 to 574 of the deduced Gal2p sequence, was isolated and subcloned in frame into the single *Eco*RI site of the vector pEx31b, which is located downstream of the *MS2* gene. The correct orientation of the subcloned *Eco*RI-*Xba*I fragment in the fusion vector pEx31b-GAL2 was determined by restriction analysis and further confirmed by reappearance of the unique *Eco*RI restriction site in pEx31b. *E. coli* SG936 containing plasmid pcI857 carrying the temperature-sensitive repressor cI857 and the kanamycin resistance gene was transformed with the gene fusion pEx31b-GAL2. Transformants were grown in Luria-Bertani medium containing ampicillin (50 $\mu g \cdot ml^{-1}$) and kanamycin (12.5 $\mu g \cdot ml^{-1}$) at 30°C to an optical density at 600 nm (OD_{600}) of 0.6 to 0.8, diluted 1:3 in fresh medium prewarmed to 65°C, and shifted to 42°C for 3 h. Inclusion bodies formed were prepared essentially as described elsewhere (52), resuspended in Laemmli sample buffer, boiled for 5 min at 95°C, and centrifuged. The supernatant was subjected to preparative sodium dodecyl sulfate-polyacrylamide gel electrophoresis (SDS-PAGE) with an 18% acrylamide gel. A predominant protein band of the expected size was visualized in the gel by incubation in ice-cold 0.25 M KCl for 10 min. The protein band was cut off the gel and used for electroelution. The eluate was extensively dialyzed against 20 mM NH_4CO_3, lyophilized, and resuspended in distilled water. The fusion protein (approximately 300 $\mu g \cdot ml^{-1}$) was injected into two rabbits. After 4 weeks, two additional injections were done every 2nd week with about 100 μg of the fusion protein.

Metabolic labeling and immunoprecipitation of Gal2p. For immunoprecipitation of Gal2p, wild-type and mutant strains were grown to an OD_{600} of 1.0 to 1.5 in mineral medium. After harvesting (4 min, 2,500 × *g*) and washing, cells were preincubated for 4 h in pulse medium (see above) at an OD_{600} of 3.0. Labeling was initiated by adding [^{35}S]methionine to a final concentration of 60 to 100 μCi ml^{-1} (Amersham). After 1 h of incubation, the cells were shifted into mineral medium containing 2% glucose, 10 mM nonradioactive methionine, and 0.4 mM cycloheximide (chase), samples (3 or 5 OD_{600} ml^{-1}) were taken at the times indicated, and the chase period was terminated by addition of twofold-concentrated azide stop solution (40 mM methionine, 20 mM sodium azide, 500 μg of bovine serum albumin [BSA] ml^{-1}). For cell lysis, 1 ml of the cell suspension was incubated for 10 min on ice with 150 μl of 1.85 M NaOH and 7.5% β-mercaptoethanol. Proteins were precipitated by adding 150 μl of 50% trichloroacetic acid, and the precipitates were collected by centrifugation for 10 min at 13,000 × *g*. The pellet was quickly rinsed with 1 M Tris base and resuspended in 15 μl of 40 mM Tris-HCl buffer (pH 6.8) containing 8 M urea, 5% SDS, 0.1 mM EDTA, and 1% β-mercaptoethanol. The samples were incubated for 10 min at 37°C and diluted in 1 ml of immunoprecipitation solution (IPS; 15 mM NaP_i buffer [pH 7.5] containing 150 mM NaCl, 1% Triton X-100, 0.5% deoxycholate, 1% SDS, 2 mM phenylmethylsulfonyl fluoride, and 1 μg of leupeptin, pepstatin A, aprotinin, chymostatin, and antipain ml^{-1}). Antiserum (8 μl) of Gal2p was added, and the mixture was incubated on a rotary shaker for 2 h at room temperature. Samples (100 μl) of 10% protein A-Sepharose CL-4B (Pharmacia) were added and incubated again on a rotary shaker for an additional 2 h at room temperature. The immunoprecipitates were washed twice with IPS containing 2 M urea and twice with IPS. Thereafter, the proteins were released from the protein A-Sepharose beads by the addition of Laemmli sample buffer and were incubated at 37°C for 10 min prior to electrophoresis. SDS-PAGE was carried out with 10% acrylamide gels. After electrophoresis, the gels were dried, fixed, washed with water, and treated with Amplify (Amersham) for 1 h. The gels were exposed on X-Omat K film (Kodak) at −70°C. Quantitation of autoradiograms was carried out with a Molecular Dynamics scanner.

Subcellular fractionation and Western blotting. The procedure for subcellular fractionation was based on sedimentation on sucrose gradients. Cells of the YMTA (Δ*pra1*) mutant strain growing to an OD_{600} of 1.0 to 1.5 in mineral medium containing 5% galactose and appropriate supplements were divided into two equal portions. One portion was immediately used for subcellular fractionation, whereas to the other portion cycloheximide and glucose were added to 0.4 mM and 2%, respectively. Incubation was continued at 30°C for an additional 5 h. Spheroplasting, lysis, and layering the cell suspension on top of a gradient containing 1 ml each (wt/vol) of 12, 18, 24, 30, 42, 48, and 54% sucrose and 0.5 ml of 60% sucrose in 10 mM morpholinepropanesulfonic acid (MOPS), 1 mM EDTA, and 0.8% sorbitol were carried out essentially as described by Egner et al. (14). Gradients were spun for 3 h at 34,000 rpm in an SW40 rotor (Beckman), fractionated from bottom to top, and collected in 1-ml fractions. Aliquots (75 μl) of the gradient fractions were supplemented with 25 μl of three times-concentrated SDS-PAGE sample buffer and incubated for 1 h at 37°C. The supernatants were isolated and subjected to SDS-PAGE in 10% acrylamide gels and electroblotted on nitrocellulose filters (Schleicher and Schuell). The filters were blocked in phosphate-buffered saline (PBS)-T buffer (50 mM KP_i buffer [pH 5.7], 100 mM NaCl, 0.1% Tween 20) containing 10% nonfat milk by shaking for 2 h at room temperature and were further treated with anti-Gal2p antibody (1:10,000 in PBS-T) for 1 h. After washing five times in PBS-T, the first antibody was detected by 1 h of incubation with a horseradish peroxidase-conjugated anti-goat immunoglobulin G (IgG) second antibody diluted 1:5,000 (Dianova, Hamburg, Germany) by using the ECL detection kit (Amersham). The plasma membrane H^+-ATPase Pma1p was detected by Western blotting and treatment with a polyclonal antibody at a 1:50,000 dilution (kindly obtained from R. Serrano).

Ha-Ub conjugates. For ubiquitination assays, yeast cells transformed with Ub-encoding plasmids YEp96 and YEp112 were grown in mineral medium containing 2% glucose until an OD_{600} of 1 to 2. After harvesting and washing, cells were resuspended in mineral medium containing 2% galactose and 100 μM $CuSO_4$ and were incubated for an additional 5 h. Thereafter, glucose was added (final concentration, 2%), the samples (5 $OD_{600} \cdot ml^{-1}$) were taken at the times indicated, and cell lysis, immunoprecipitation with anti-Gal2p antibody, SDS-PAGE, and electroblotting were performed as described above. The nitrocellulose filters were blocked as described above and gently treated for 2 h with Ha antibodies (Babco, Inc.; 1:5,000 in PBS-T). After washing four times in PBS-T, secondary antibody (anti-mouse IgG; Dianova) was added (1:5,000 in PBS-T), and the mixture was incubated for 1 h. Ha-Ub conjugates were visualized with the ECL detection kit (Amersham).

Immunofluorescence. For indirect fluorescence, cells of the YMTA (Δ*pra1*) mutant strain growing logarithmically in mineral medium containing 5% galactose and supplements were divided into two equal portions. One portion was used immediately for immunofluorescence detection of Gal2p. The other portion was treated with 2% glucose and 0.4 mM cycloheximide for 5 h prior to immunofluorescence measurements. Prior to immunofluorescence, cells were fixed in the medium with 3.7% formaldehyde for 2 h. Spheroplasting and antibody staining were performed as described by Pringle et al. (39), with the exception that the fixed spheroplasts were permeabilized in spheroplasting buffer containing 0.1% Triton X-100 for 5 min at room temperature. Anti-Gal2p antibodies were purified prior to use by immunoadsorption with spheroplasts of a Δ*gal2* strain. Colocalization experiments with purified anti-Gal2p and mouse anti-yeast monoclonal carboxypeptidase yscY (CPY) antibody (Molecular Probes) were carried out with both primary antibodies present concomitantly in incubation mixtures. Both secondary antibodies were simultaneously present in secondary incubation mixtures. Primary and secondary antisera were diluted in PBS containing BSA and 0.1% Triton X-100 as follows: Gal2p antibody, 1:50; carboxypeptidase yscY antibody, 1:500. Secondary fluorescent antibodies were diluted as follows: fluorescein isothiocyanate-conjugated goat anti-rabbit IgG, 1:500; and Cy3-conjugated anti-mouse IgG (Molecular Probes), 1:500. As controls for colocalization experiments, one or the other primary antibody was omitted from the primary incubation mixture. In addition, a Δ*gal2* strain was used as a control. For DNA staining, the fluorescent DNA-binding dye 4′,6′-diamidino-2-phenylindole (DAPI) was added to the mounting medium at 10 $\mu g \cdot ml^{-1}$. Cells were visualized with a Zeiss Axioscop and photographed by using Kodak Tmax 400 film.

Enzyme and transport assays. For measurement of NADPH-cytochrome *c* oxidoreductase, the reaction mixture consisted of 100 mM KP_i (pH 7.5), 1 mM KCN, 1 μM flavin mononucleotide, 0.1% Triton X-100, 0.1% cytochrome *c*, and 0.25 mM NADPH. Volumes of 25 to 50 μl of the gradient fractions were added, and the increase in absorbance at 550 nm was monitored. Vacuolar α-mannosidase was assayed with *p*-nitrophenyl mannoside as the substrate following the generation of *p*-nitrophenol. To a 250-μl reaction mixture consisting of 100 mM morpholineethanesulfonic acid (MES)-NaOH (pH 6.5), 0.2% Triton X-100, and 1 mM *p*-nitrophenyl mannoside, 50 μl of the gradient fractions was added. After incubation at 30°C for 1 h, the reaction was stopped by addition of 2 volumes of 2% Na_2CO_3. For galactose transport measurements, 1 ml of yeast culture portions, taken at the indicated times of inactivation, was incubated with 4 mM [^{3}H]galactose for 30 and 60 s at 30°C and was rapidly filtered through Millipore HA filters (filter size, 0.45 μm). The filters were quickly washed twice with ice-cold water, and the radioactivity taken up by cells was measured in a liquid scintillation counter.

RESULTS

Immunological identification of the Gal2 transporter. The Gal2 transporter was monitored with polyclonal antibody against an MS2-Gal2 fusion protein. Cellular protein extracts of pulse-labeled wild-type strain WCG4 were treated with antibody. Immunoblot analysis revealed that in cells induced for Gal2p synthesis, a major protein band migrating at 47 to 48

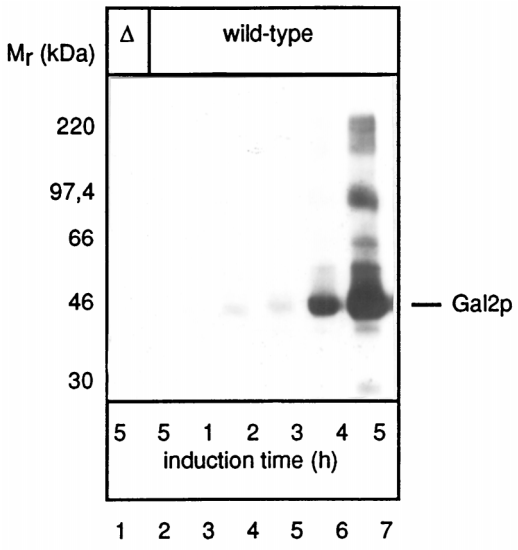

FIG. 1. Immunodetection of the Gal2 transporter. Wild-type WCG4α cells and cells of the Δ*gal2* deletion strain (Δ), grown overnight on mineral-glucose (2%) medium, were harvested, washed, and transferred to mineral-galactose (5%) medium to induce Gal2p synthesis. The cell samples, taken at different times of induction, were pulse-labeled with [^{35}S]methionine for 1 h, cell extracts were prepared, and immunoprecipitation with Gal2p antibodies, SDS-PAGE, and autoradiography were followed as described in Materials and Methods (lanes 1 and 3 to 7). For an additional control, wild-type strain WCG4α was pulse-labeled with [^{35}S]methionine after 4 h in mineral-raffinose (2%) medium (lane 2).

kDa appeared with increasing intensity during the 5-h induction period (Fig. 1, lanes 3 to 7). The molecular mass of Gal2p predicted on the basis of the *GAL2* gene sequence is 63.7 kDa (37, 53). Verification that the 47- to 48-kDa protein band found represents the *GAL2* gene product was obtained by showing that immunoreactive material was produced neither in wild-type cells growing under noninducing conditions of 2% raffinose as the sole carbon source (Fig. 1, lane 2) nor in Δ*gal2* cells (Fig. 1, lane 1). The reason for the discrepancies between the predicted and estimated molecular masses of Gal2p is not known. The lower molecular mass can be best explained by an aberrant mobility of the protein on SDS-PAGE due to the hydrophobic character of Gal2p. Similar differences in molecular masses were found for the yeast Mal61 (56), Hxt2 (58), and Fur4 (51) transporters. In addition, extracts of induced cells contained protein bands with higher apparent molecular masses. (Fig. 1). There is evidence suggesting that these species represent aggregates of Gal2p or aggregates with other cell constituents. (i) Heat treatment (3 min, 95°C) increased the amount of various higher-molecular-mass species, accompanied by the nearly complete disappearance of the 47- to 48-kDa Gal2p (not shown). (ii) The higher-molecular-mass species were not modified by endo-β-*N*-acetylglucosaminidase H treatment under conditions which led to complete deglycosylation of a control protein, carboxypeptidase yscY (data not shown). (iii) The higher-molecular-mass species were missing in the Δ*gal2* control strain (Fig. 1, lane 1).

Catabolite inactivation of the Gal2 transporter. The maximum capacity of Gal2p-mediated substrate transport rapidly decreases when cytosolic protein synthesis is impaired and a readily fermentable carbon source is added to cells (11, 35). We carried out pulse-labeling analysis to show whether this results from an increased turnover rate of Gal2p. We incubated cells for 5 h on galactose and examined the fate of Gal2p

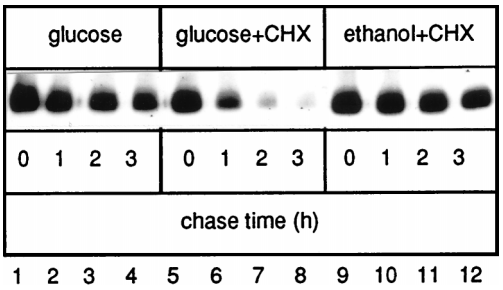

FIG. 2. Gal2p is metabolically unstable. Wild-type WCG4α cells induced for Gal2p synthesis for 4 h were pulse-labeled for 1 h with [^{35}S]methionine and shifted to glucose (lanes 1 to 4), glucose and cycloheximide (CHX) (lanes 5 to 8), and ethanol and cycloheximide (lanes 9 to 12) containing mineral medium and 10 mM nonradioactive methionine for the times indicated. Samples were taken and cell extracts were treated as described in the legend to Fig. 1.

by immunoblot analysis under different chase conditions (Fig. 2). As can be seen in Fig. 2, lanes 5 to 8, Gal2p disappeared most rapidly on account of the concomitant presence of glucose and cycloheximide in the medium. In addition, glucose alone led to the disappearance of Gal2p, but to a lesser extent (Fig. 2, lanes 1 to 4). Ethanol and cycloheximide (Fig. 2, lanes 9 to 12) were least effective in promoting this process. Galactose plus cycloheximide had no effect (not shown). The half-lives of Gal2p were estimated as about 1 h in glucose and cycloheximide-containing medium, 3.5 h in glucose-containing medium, and longer than 5 h in medium containing ethanol and cycloheximide (Table 1). In addition, inactivation of Gal2p was completely inhibited when 5 mM sodium azide was added to the medium prior to the addition of glucose and cycloheximide (data not shown). These data are completely consistent with results of earlier studies of galactose transport under different growth conditions (11, 35) and clearly show that proteolytic degradation of Gal2p is the reason for impairment of galactose transport when glucose or glucose and cycloheximide are added to cells growing on galactose. This degradation process apparently requires a source of metabolic energy. With a loss of transport capacity of 48% after 1 h, 71% after 2 h, and 86% after 3 h, these numbers nicely reflect the disappearance of Gal2p in the presence of glucose and cycloheximide.

Vacuolar but not cytoplasmic proteolysis is responsible for degradation of the Gal2 transporter. Two major cellular protein degradation pathways, a cytoplasmic pathway and a vacuolar pathway, exist in yeast. The cytoplasmic proteolytic system is represented by the 26S proteasome, an ATP-dependent multisubunit enzyme complex, which degrades multiubiquiti-

TABLE 1. Half-lives of Gal2p in different strains under different inactivation conditions[a]

Strain	Relevant genotype	Condition	Half-life of Gal2p (h)
WCG4α	Wild type	Glucose	3.5
		Glucose + CHX	1.0
		Ethanol + CHX	>5.0
WCG4α	Wild type	Glucose + CHX	1.0
WCG4-11/21	*pre1-1 pre2-2*	Glucose + CHX	1.0
WCG4α	Wild type	Glucose + CHX	1.0
YMTA	Δ*pra1*	Glucose + CHX	3.0
RH144-3D	Wild type	Glucose + CHX	2.0
RH266-1D	*end 3*	Glucose + CHX	6.0
RH268-1C	*end 4*	Glucose + CHX	>10.0

[a] Gal2p signals of the autoradiograms were quantified by densitometry. CHX, cycloheximide.

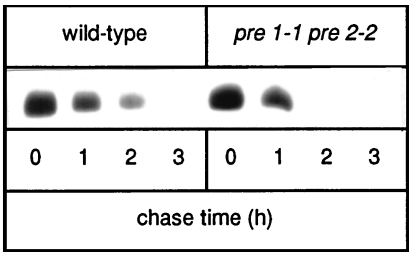

FIG. 3. Gal2p instability is not affected in a proteasome-defective *pre1-1 pre2-2* mutant. Strains WCG4α (wild-type) and WCG4-11/22 (*pre1-1 pre2-2*) were grown, induced for Gal2p synthesis, and pulse-labeled as described in the legend to Fig. 2. Thereafter, the cells were treated with glucose and cycloheximide as well as 10 mM nonradioactive methionine for the times indicated. Samples were taken and cell extracts were treated as described in the legend to Fig. 1.

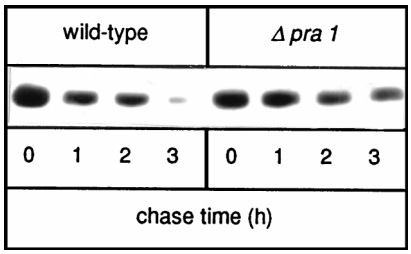

FIG. 4. Gal2p is stabilized in a vacuolar proteinase-defective mutant. Pulse-chase analysis of WCG4α (wild-type) and YMTA (Δ*pra1*) induced for Gal2p synthesis was done as described in the legend to Fig. 3.

nated proteins (22–24). The possible involvement of this proteasome in the degradation of Gal2p was examined by using strains harboring missense mutations in two essential proteasomal genes, *PRE1* and *PRE2*, which both encode β-subunits of the proteasome responsible for the chymotrypsin-like activity of the enzyme complex (18, 19). Pulse-chase labeling, immunoprecipitation, and SDS-PAGE of extracts from wild-type and isogenic *pre1-1 pre2-2* double mutant WCG4-11/21 cells induced for 5 h for Gal2p synthesis and thereafter treated with glucose and cycloheximide showed that the degradation of Gal2p was not altered in the mutant strain compared to the wild type (Fig. 3 and Table 1). Analogous data were also obtained when Gal2 transport activity in mutant and wild-type strains was measured under the same experimental conditions (not shown). Since the *pre1-1 pre2-2* mutant is defective only in chymotryptic activity, leaving the two other activities of the proteasome intact, we also examined Gal2p transport activity in strains carrying temperature-sensitive mutations in the *CIM3* and *CIM5* genes, which encode regulatory subunits of the proteasome (17). In both mutants, the Gal2p transport activity was found to be of the wild-type level (data not shown).

The vacuole, representing the second major site of cellular protein degradation, contains a number of peptidases of which proteinase yscA, the *PRA1/PEP4* gene product, occupies a central position (26, 28). This proteinase is essential for initiation of its own processing and activation as well as maturation and activation of several other major vacuolar proteinases. Thus, an inactive proteinase yscA leads to a proteolytically inactive vacuole (54). Therefore, if degradation of Gal2p occurred in the vacuole, it should be stabilized in a proteinase yscA (Δ*pra1*) mutant strain. We examined this possibility by measuring the changes in the level of Gal2p in a galactose-induced and catabolite-inactivated Δ*pra1* mutant strain (YMTA) and, for comparison, in a wild-type strain via pulse-chase analysis. As shown in Fig. 4 (lanes 5 to 8) and Table 1, the decrease in the amount of Gal2p under catabolite inactivation conditions is reduced by at least threefold in the mutant compared to the wild-type strain WCG4α (Fig. 4, lanes 1 to 4, and Table 1). These data demonstrate that the turnover of Gal2p is not mediated by the proteasome but is dependent on the vacuolar proteolytic machinery. This implies that Gal2p is delivered from the plasma membrane to the vacuole.

The Gal2 transporter accumulates in the vacuole of a Δ*pra1* mutant strain. In order to obtain more direct evidence of Gal2p delivery to the vacuole triggered by the catabolite inactivation process, we examined its changes in intracellular distribution by indirect immunofluorescence microscopy and subcellular fractionation. Using both approaches, we compared the intracellular distribution of Gal2p in a Δ*pra1* mutant strain before and after 5 h of glucose inactivation. Staining of Gal2p by indirect fluorescence revealed a rim pattern at time zero of inactivation in cells, which is typical for plasma membrane proteins (Fig. 5A), whereas after a 5-h inactivation period, a significant portion of Gal2p staining occurs in vacuoles or exhibits a perivacuolar pattern (Fig. 5B). The vacuole was identified by Nomarski optics (Fig. 5E and F). The staining is specific for Gal2p, since no staining of the internal contents of the cell was observed when a Δ*gal2* control strain was stained or when anti-Gal2p antibody was omitted from incubation mixtures (data not shown). The following observations are consistent with the vacuolar location of Gal2p after 5 h of inactivation: (i) immunostaining of carboxypeptidase yscY, a typical marker enzyme of the vacuole, colocalizes with Gal2p (Fig. 5C and D); and (ii) DNA staining with DAPI (Fig. 5G and H) excludes association of Gal2p with the nucleus or with the mitochondria.

The delivery of Gal2p into the vacuole triggered by its catabolite inactivation was further confirmed by subcellular localization as analyzed by density gradient centrifugation. Cell extracts prepared from gently lysed spheroplasts of a Δ*pra1* mutant strain induced for 5 h for synthesis of Gal2p were loaded onto a sucrose gradient. All fractions collected were assayed for the presence of Gal2p and the plasma membrane marker Pma1p by SDS-PAGE and immunoblot analysis. In addition, the activities of marker enzymes of the vacuoles (α-mannosidase) and the endoplasmic reticulum (ER) (NADPH-cytochrome *c* oxidoreductase) were assayed. At time zero of catabolite inactivation, the bulk of Gal2p equilibrates together with Pma1p at sucrose concentrations of between 50 and 40% (Fig. 6A, fractions 3 and 4 and Fig. 6C). This fraction is clearly separated from the ER and the vacuolar markers (Fig. 6D) that migrate mainly in a density range of 30 to 15% sucrose (Fig. 6D, fractions 6 to 9). After 5 h of inactivation, Gal2p is predominantly associated with the internal membranes that migrate with the major peak of vacuolar α-mannosidase activity (Fig. 6B, lanes 6 to 8).

Degradation of the Gal2 transporter is dependent on the *END3* and *END4* gene products. Proteins degraded in the vacuole reach this organelle by endocytosis or autophagocytosis, the first pathway being responsible for transport of plasma membrane and extracellular proteins to this degradative organelle (28, 45). Two mutants of *S. cerevisiae* with defects in genes necessary for endocytosis, *END3* and *END4*, had been isolated (41, 45) and shown to be involved in the first steps of the endocytic pathway. It had been shown that these gene products are needed for internalization of the pheromone receptors Ste2p and Ste3p (10, 46) and at least five plasma membrane transport proteins, as are Itr1p (32), Fur4p (57), Mal61p (36, 43), Ste6p (2, 29), and Pdr5p (14). We thus ex-

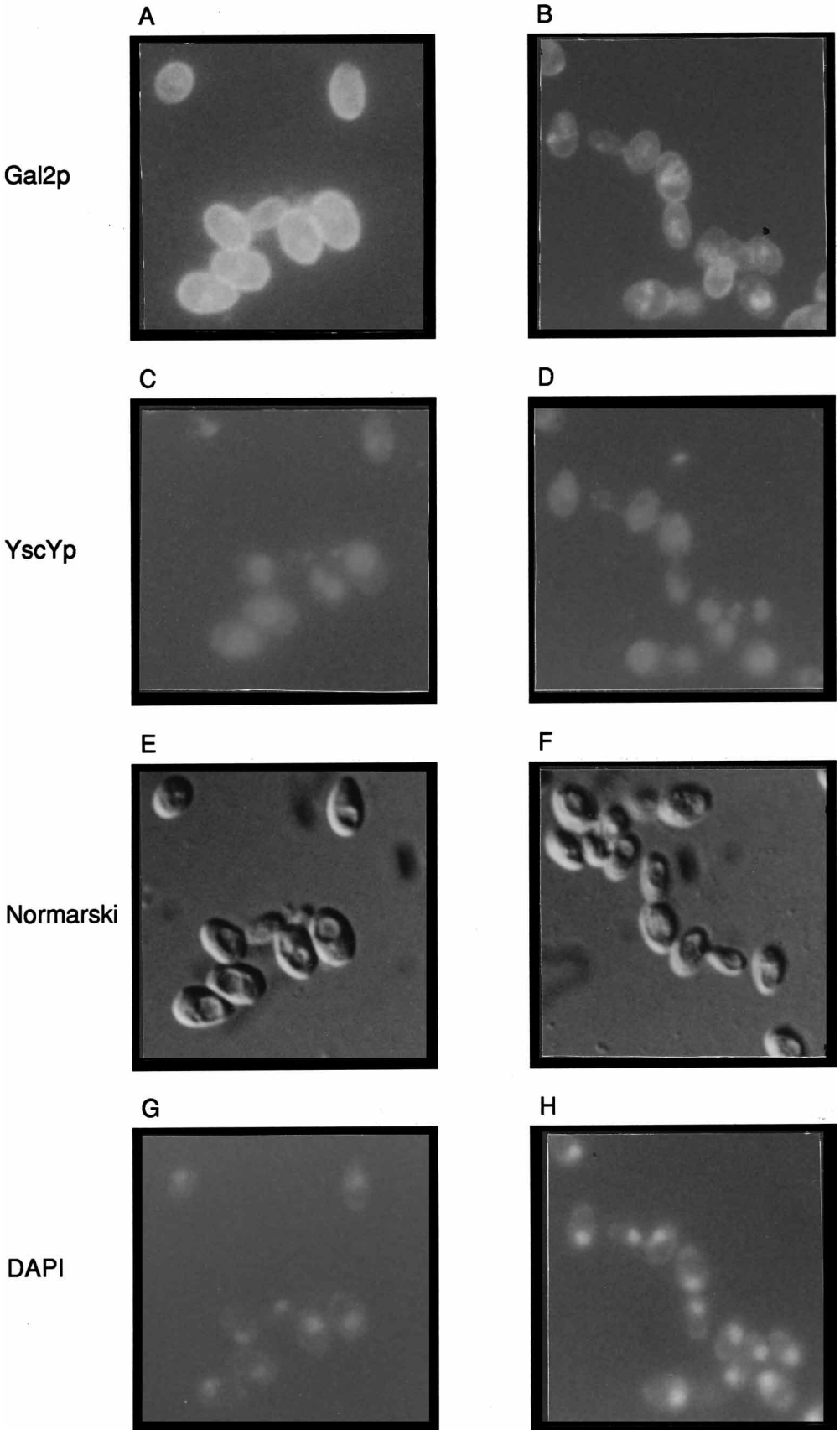

FIG. 5. Indirect immunofluorescence of Gal2p and carboxypeptidase yscY before and after catabolite inactivation. The mutant strain YMTA (Δ*pra1*) was induced for 5 h for Gal2p synthesis. Cells were taken immediately after induction (A, C, E, and G) or were treated with glucose and cycloheximide for 5 h (B, D, F, and H). Thereafter, they were fixed and prepared for immunofluorescence measurements as described in Materials and Methods. The cells were stained with antibodies against Gal2p (A and B) and carboxypeptidase yscY (C and D). Visualization of vacuoles (E and F) and DNA (G and H) was performed with Nomarski optics and DAPI, respectively.

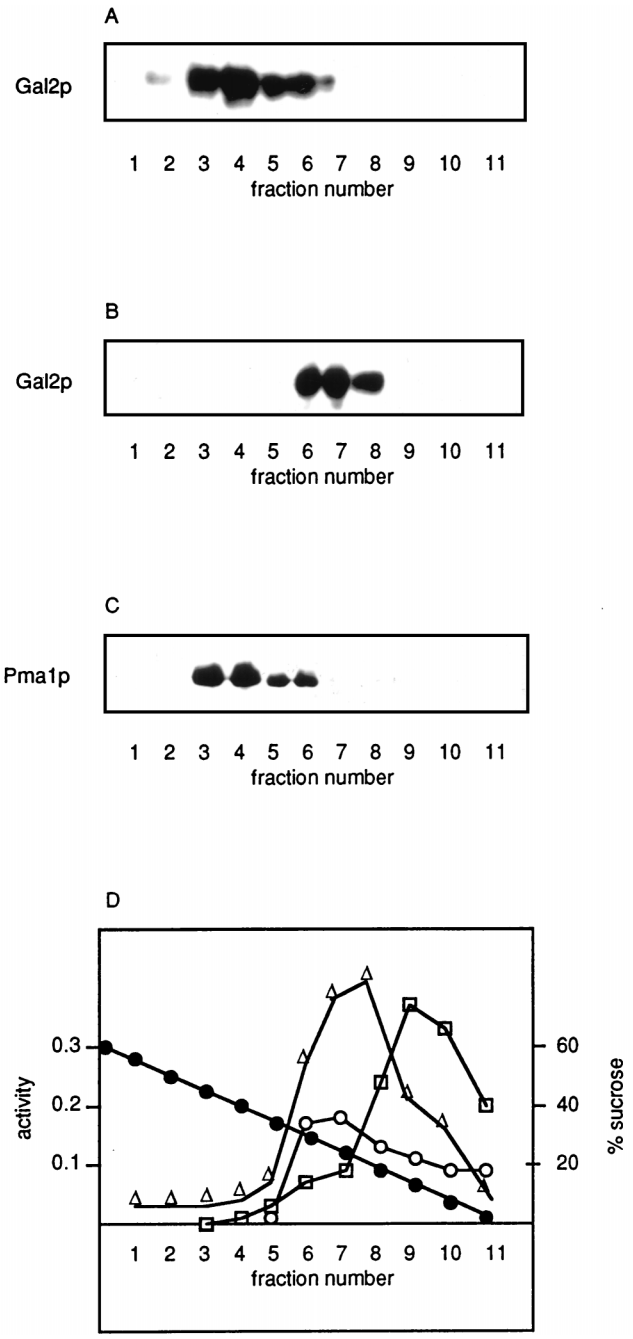

FIG. 6. Subcellular distribution of Gal2p before and after catabolite inactivation. The mutant strain YMTA (Δ*pra1*) was induced for 5 h for Gal2p synthesis, and samples were treated 5 h without (A) or with (B) glucose and cycloheximide as described in the legend to Fig. 5. Cell extracts were layered on a 12 to 60% sucrose gradient, and subcellular organelles were separated after 3 h of centrifugation at 150,000 × *g* as described in Materials and Methods. Aliquots of the gradient fractions were separated on SDS-PAGE and were analyzed by Western blotting with Gal2p antiserum. (C) For control of plasma membrane proteins, fractions were treated with Pma1p antibodies. (D) α-Mannosidase activity (Δ) as the vacuolar marker and NADPH-cytochrome *c*-oxidoreductase (○) as the ER marker (both activities expressed in arbitrary units), density (percent sucrose [wt/vol] [●]), and protein concentrations (□) were plotted against the fraction number.

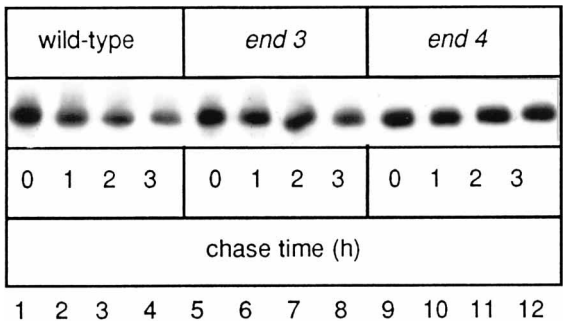

FIG. 7. Gal2p is stabilized in endocytosis-defective mutants. Induction and pulse-labeling analysis of Gal2p in strains RH144-3D (wild-type [lanes 1 to 4]), RH266-1D (*end3* [lanes 5 to 8]), and RH268-1C (*end4* [lanes 9 to 12]) were performed at 24°C as described in the legend to Fig. 1. Thereafter, treatment with glucose and cycloheximide was done at the times indicated at the nonpermissive temperature of 37°C. Immunoprecipitation, SDS-PAGE, and autoradiography were done as described in Materials and Methods.

amined the fate of Gal2p using the temperature-sensitive *end3* and *end4* mutants, which express a defect in internalization of all of the proteins indicated above at the nonpermissive temperature of 37°C. Cells expressing Gal2p were pulse-labeled with [^{35}S]methionine at the permissive temperature of 24°C and chased under catabolite inactivation conditions with nonradioactive methionine at the nonpermissive temperature for the time intervals indicated. Analysis of the radioactive, immunoprecipitated Gal2p revealed that the transporter is partly stabilized in the *end3* mutant (Fig. 7, lanes 5 to 8) and is completely stabilized in the *end4* mutant (Fig. 7, lanes 9 to 12). The estimated half-lives of Gal2p were about 2 h for the wild type, 6 h for *end3*, and more than 10 h for the *end4* strains (Table 1). These data clearly demonstrate that glucose- and cycloheximide-triggered degradation of Gal2p is dependent on endocytosis.

Gal2p is ubiquitinated. Until recently (20), it was believed that ubiquitination targeted proteins only to degradation via the cytoplasmic and nuclearly located proteasome (22–24). Examples for proteasome-mediated degradation of ubiquitinated proteins are the MATα2 repressor (44), catabolite-inactivated fructose-1,6-bisphosphatase (48), and misfolded ER membrane proteins (44), as well as misfolded luminal ER proteins (21). The finding that plasma membrane proteins are ubiquitinated prior to their delivery into the vacuole (13, 16, 20, 29) prompted us to examine if ubiquitination also occurs in the case of Gal2p and thus is probably a more general feature of plasma membrane proteins, whose final destination is the vacuole. We overexpressed a functional version of Ha epitope-tagged ubiquitin in wild-type cells expressing Gal2p and in Δ*gal2* cells before and after induction of catabolite inactivation. Crude extracts from glucose-inactivated cells either transformed with plasmid YEp96 expressing wild-type Ub or plasmid YEp112 expressing Ha-Ub were immunoprecipitated with anti-Gal2p antibodies, and proteins were separated by SDS-PAGE and blotted onto nitrocellulose filters. Thereafter, the filters were probed with Ha antibodies. Putative Ub-Gal2 conjugates were detected by enhanced chemiluminescence. As can be seen in Fig. 8, extracts from wild-type cells expressing Ha-Ub exhibit no ubiquitinated Gal2 material prior to inactivation (Fig. 8, lane 1), while a complex set of Ha-Ub-Gal2 conjugates can be obtained after shifting the cells to glucose (Fig. 8, lanes 2 to 4). The amount of ubiquitinated Gal2 material increases for up to 30 min after glucose addition (Fig. 8, lanes 1 to 3), followed by a drastic decrease (Fig. 8, lane 4)

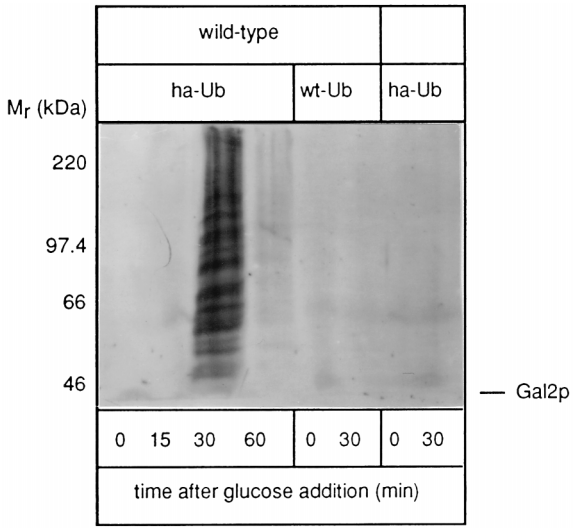

FIG. 8. Immunodetection of ubiquitin-Gal2p conjugates during catabolite inactivation. Extracts prepared from cells induced for Gal2p synthesis and overexpressing Ha-Ub or wild-type ubiquitin (wt-Ub) were immunoprecipitated with Gal2p antibodies, separated by SDS-PAGE, electroblotted onto nitrocellulose, and probed with Ha antibodies. Ha-Ub-Gal2p conjugates occur after shifting the cells onto glucose (lanes 1 to 4). The control wild-type cells (*GAL2*) expressing wild-type Ub (lanes 5 and 6) and Δ*gal2* mutant cells expressing Ha-Ub (lanes 7 and 8) display no Gal2p-Ub conjugates.

after 60 min of inactivation. This behavior is consistent with the view that Gal2p is ubiquitinated upon the onset of glucose-triggered inactivation. The absence of these higher-molecular-mass bands in cells expressing wild-type ubiquitin (Fig. 8, lanes 5 and 6) and in Δ*gal2* mutant cells expressing Ha-Ub (Fig. 8, lanes 7 and 8) before and after 30 min of glucose addition confirms that the bands observed in Fig. 8 represent ubiquitinated forms of Gal2p.

DISCUSSION

Based on transport studies (11, 40) and the highly hydrophobic character of the protein deduced from the DNA sequence (37, 53), Gal2p has been proposed to function as a major galactose-specific plasma membrane transporter. We show that Gal2p is a plasma membrane-localized protein by subcellular fractionation and indirect immunofluorescence using polyclonal antibodies raised against recombinant Gal2 transporter protein (Fig. 5 and 6). Previous data indicating that β-galactosidase activity of a *GAL2-lacZ*-encoded fusion protein copurifies with a membrane fraction enriched for the plasma membrane (55) are consistent with our findings of plasma membrane localization of the Gal2 transporter.

Although Gal2p is a rather stable protein in cells growing on galactose as the sole carbon source with a half-life of more than 15 h (data not shown), its activity is rapidly impaired upon addition of glucose to the growth medium (reference 11 and our unpublished data). Using pulse-chase analysis and immunodetection, we demonstrate that the observed decrease in Gal2p transport activity upon glucose addition is due to proteolytic degradation of the Gal2 transporter. The degradation rate of Gal2p correlates with the decrease in galactose transport capacity. We show that glucose-induced proteolysis of Gal2p is 3.5-fold accelerated in the presence of cycloheximide, an inhibitor of cytosolic protein synthesis (Fig. 2). Recently, Chiang et al. (9) reported that glucose-triggered Gal2p degradation does not occur in the presence of cycloheximide and suggested that Gal2p degradation requires synthesis of some new protein. This is in contrast to our findings and earlier data of Busturia and Lagunas (5, 6) and DeJuan and Lagunas (11), who report an increased efficiency of inactivation of glucose, galactose, and maltose transport triggered by glucose upon inhibition of protein synthesis. In no case was a negative effect of cycloheximide on inactivation of galactose transport reported. Whether the discrepancies are due to strain differences, different conditions of cell cultivation, or other factors remains to be seen. In any case, Gal2p may be added to the list of short-lived proteins whose half-lives are dependent on cellular signalling and range from about 1 min to 1.5 h. To date, this group of proteins includes transporters that mediate specific transport of maltose and other disaccharides (Mal11p and Mal61p [7, 33, 36]), inositol (Itr1p [31, 32]), uracil (Fur4p [57]), **a**-pheromone (Ste6p [2, 29]), and some unwanted drugs (Pdr5p [14]) or that serve as the **a**- and α-pheromone receptors (10, 20).

There exist two major proteolytic systems in yeast. One is represented by the 26S proteasome complex located in the cytoplasm and nucleus (22–24). It is composed of two multisubunit components, the catalytic 20S proteasome core that contains the proteolytic activities of the complex, and a 19S complex, harboring isopeptidase activity, a ubiquitin-conjugate binding component and subunits bearing ATPase activities. Yeast proteasome mutants are unable to degrade cytosolic proteins specifically tagged for degradation, such as the transcriptional regulator MATα2 (44), catabolite-inactivated fructose-1,6-bisphosphatase (47, 48), a key enzyme in gluconeogenesis, misfolded proteins of the ER membrane (3), the ER lumen (21), and probably many others (1, 12, 27, 30, 34, 49, 50, 59). A defect in the proteasome results in accumulation of the proteins listed above. Using proteasome-defective mutants, we can clearly demonstrate that Gal2 transporter stability is not affected in mutants with defects in either the catalytic (*pre1-1 pre2-2* [Fig. 2]) or the regulatory (*cim3-1 cim5-1* [data not shown]) activities of the protease complex. Hence, the proteasome is apparently not involved in degradation of the Gal2 transporter under catabolite-inactivation conditions. Using strains harboring mutations in the *END3*, *END4*, and *PRA1*/*PEP4* genes, we demonstrate that Gal2p must be endocytosed and requires an active vacuole to undergo catabolite-stimulated degradation. Mutants conditionally defective in *end3*, *end4*, or *pra1/pep4-3* show a three- to sixfold-increased stability upon catabolite inactivation conditions as compared to wild-type strains (Fig. 4 and 7; Table 1). Moreover, delivery of Gal2p to the vacuole and its accumulation therein triggered by glucose were clearly demonstrated by indirect fluorescence (Fig. 5) and subcellular fractionation (Fig. 6) in a mutant YMTA strain deficient in proteinase yscA, a key enzyme of the vacuolar degradation machinery. Similarly, degradation of Mal61p (36, 43), Pdr5p (14), Ste6p (29), Ste2p (20), and Fur4p (16, 57) is not dependent on the 26S proteasome. All available data show that the above-mentioned yeast plasma membrane proteins may share a degradation pathway, involving their release from the membrane and delivery to the vacuole via endocytosis.

For Pdr5p (13), Ste6p (29), Fur4p (16), and Ste2p (20), ubiquitination prior to endocytosis and degradation in the vacuole has been reported. Using overexpression of a Ha-tagged version of ubiquitin, we were able to show that Gal2p is also ubiquitinated under catabolite inactivation conditions (Fig. 8). It has been shown that ubiquitination is a prerequisite for internalization and subsequent vacuolar proteolysis of Fur4p (16). On the basis that all endocytosed vacuolarly delivered plasma membrane proteins are ubiquitinated, one might spec-

ulate that ubiquitination is a general mechanism to select plasma membrane proteins for endocytosis and degradation in the vacuole.

It is interesting to note that ubiquitination of cytoplasmic proteins and proteins of the ER membrane leads to their recognition by the 26S proteasome, leading to subsequent degradation by this particle, while ubiquitination of plasma membrane proteins is neglected by the proteasome and induces a selective endocytic process instead. It will be of high interest to distinguish the mechanistic details which lead to the two different pathways.

ACKNOWLEDGMENTS

We thank H.-L. Chiang, M. Hochstrasser, C. Mann, H. Riezman, and H. Ronne for kindly providing strains and plasmids. Thanks are due to R. Serrano for Pma1-directed antibodies, M. Knop for help with the immunofluorescence experiments, and S. Schork for much advice.

This work was supported by the Deutsche Forschungsgemeinschaft, Bonn, Germany, the Chemische Industrie, Frankfurt, Germany and grant no. 204/96/1315 of the Grant Agency of the Czech Republic.

REFERENCES

1. **Amon, A., S. Irniger, and K. Nasmyth.** 1994. Closing the cell cycle circle in yeast: G2 cyclin proteolysis initiated at mitosis persists until the activation of G1 cyclins in the next cycle. Cell **77:**1037–1050.
2. **Berkower, C., D. Loyaza, and S. Michaelis.** 1994. Metabolic instability and constitutive endocytosis of STE6, the **a**-factor transporter of *Saccharomyces cerevisiae*. Mol. Biol. Cell **5:**1185–1198.
3. **Biederer, T., C. Volkwein, and T. Sommer.** 1996. Degradation of subunits of the Sec61p complex, an integral component of the ER membrane, by the ubiquitin-proteasome pathway. EMBO J. **15:**2069–2076.
4. **Bisson, L. F., D. M. Coons, A. L. Kruckeberg, and D. A. Lewis.** 1993. Yeast sugar transporters. Crit. Rev. Biochem. Mol. Biol. **28:**259–308.
5. **Busturia, B., and R. Lagunas.** 1985. Identification of two forms of the maltose transport system in *Saccharomyces cerevisiae* and their regulation by catabolite inactivation. Biochim. Biophys. Acta **820:**324–326.
6. **Busturia, B., and R. Lagunas.** 1986. Catabolite inactivation of the glucose transport system in *Saccharomyces cerevisiae*. J. Gen. Microbiol. **132:**379–385.
7. **Cheng, Q., and C. A. Michels.** 1991. *MAL11* and *MAL61* encode the inducible high-affinity maltose transporters in *Saccharomyces cerevisiae*. J. Bacteriol. **173:**1871–1820.
8. **Chiang, H.-L., and R. Schekman.** 1991. Regulated import and degradation of a cytosolic protein in the yeast vacuole. Nature **350:**313–318.
9. **Chiang, H.-L., R. Schekman, and S. Hamamoto.** 1996. Selective uptake of cytosolic, peroxisomal, and plasma membrane proteins into the yeast lysosome for degradation. J. Biol. Chem. **271:**9934–9941.
10. **Davis, N. G., J. L. Horecka, and G. F. Sprague.** 1993. *cis*- and *trans*-acting function required for endocytosis of the yeast pheromone receptors. J. Cell. Biol. **122:**53–65.
11. **DeJuan, C., and R. Lagunas.** 1986. Inactivation of the galactose transport system in *Saccharomyces cerevisiae*. FEBS Lett. **207:**258–261.
12. **Deshaies, R. J., V. Chau, and M. Kirschner.** 1995. Ubiquitination of the G1 cyclin Cln2p by a Cdc34p-dependent pathway. EMBO J. **14:**303–312.
13. **Egner, R., and K. Kuchler.** 1996. The yeast multidrug transporter Pdr5p of the plasma membrane is ubiquitinated prior to endocytosis and degradation in the vacuole. FEBS Lett. **378:**177–181.
14. **Egner, R., Y. Mahe, R. Pandjaitan, and K. Kuchler.** 1995. Endocytosis and vacuolar degradation of the plasma membrane-localized Pdr5p ATP-binding cassette multidrug transporter in *Saccharomyces cerevisiae*. Mol. Cell. Biol. **15:**5879–5887.
15. **Ellison, M. J., and M. Hochstrasser.** 1991. Epitope-tagged ubiquitin. A new probe for analyzing ubiquitin function. J. Biol. Chem. **266:**21150–21157.
16. **Galan, J. M., C. Volland, D. Urban-Grimal, and R. Hagenauer-Tsapis.** 1994. The yeast plasma membrane uracil permease is stabilized against stress induced degradation by a point mutation in a cyclin-like "destruction box". Biochem. Biophys. Res. Commun. **201:**769–775.
17. **Ghislain, M., A. Udvardy, and C. Mann.** 1993. *S. cerevisiae* 26S protease mutants arrest cell division in G2/metaphase. Nature **366:**358–362.
18. **Heinemeyer, W., J. A. Kleinschmidt, J. Saidowsky, C. Escher, and D. H. Wolf.** 1991. Proteinase yscE, the yeast proteasome/multicatalytic-multifunctional proteinase: mutants unravel its function in stress induced proteolysis and uncover its necessity for cell survival. EMBO J. **10:**555–562.
19. **Heinemeyer, W., A. Gruhler, V. Mohrle, Y. Mahe, and D. H. Wolf.** 1993. *PRE2*, highly homologous to the human major histocompatibility complex-linked *RING10* gene, codes for a yeast proteasome subunit necessary for chymotryptic activity and degradation of ubiquitinated proteins. J. Biol. Chem. **268:**5115–5120.
20. **Hicke, L., and H. Riezman.** 1996. Ubiquitination of a yeast plasma membrane receptor signals its ligand-stimulated endocytosis. Cell **84:**277–287.
21. **Hiller, M. M., A. Finger, M. Schweiger, and D. H. Wolf.** 1996. ER degradation of a misfolded luminal protein by the cytosolic ubiquitin-proteasome pathway. Science **273:**1725–1728.
22. **Hilt, W., and D. H. Wolf.** 1995. Proteasomes of the yeast *S. cerevisiae*: genes, structure and functions. Mol. Biol. Rep. **21:**3–10.
23. **Hilt, W., and D. H. Wolf.** 1996. Proteasomes: destruction as a programme. Trends Biochem. Sci. **21:**96–102.
24. **Hochstrasser, M.** 1995. Ubiquitin, proteasomes, and the regulation of intracellular protein degradation. Curr. Opin. Cell Biol. **7:**215–223.
25. **Holzer, H.** 1976. Catabolite inactivation in yeast. Trends Biochem. Sci. **1:**178–181.
26. **Jones, E. W.** 1991. Three proteolytic systems in the yeast *Saccharomyces cerevisiae*. J. Biol. Chem. **266:**7963–7966.
27. **Kaplon, T., and M. Jacquet.** 1995. The cellular content of Cdc25p, the Ras exchange factor in *Saccharomyces cerevisiae*, is regulated by destabilization through a cyclin destruction box. J. Biol. Chem. **270:**20742–20747.
28. **Knop, M., H. H. Schiffer, S. Rupp, and D. H. Wolf.** 1993. Vacuolar/lysosomal proteolysis: proteases, substrates, mechanisms. Curr. Opin. Cell Biol. **5:**990–996.
29. **Kolling, R., and C. P. Hollenberg.** 1994. The ABC-transporter Ste6 accumulates in the plasma membrane in a ubiquitinated form in endocytosis mutants. EMBO J. **13:**3261–3271.
30. **Kornitzer, D., B. Raboy, R. G. Kulka, and G. R. Fink.** 1994. Regulated degradation of the transcriptional factor Gcn4. EMBO J. **13:**6021–6030.
31. **Lai, K., and P. McGraw.** 1994. Dual control of inositol transport in *Saccharomyces cerevisiae* by irreversible inactivation of permease and regulation of permease synthesis by *INO2*, *INO4*, and *OPI1*. J. Biol. Chem. **269:**2245–2251.
32. **Lai, K., P. Bolognese, S. Swift, and P. McGraw.** 1995. Regulation of inositol transport in *Saccharomyces cerevisiae* involves inositol-induced changes in permease stability and endocytic degradation in the vacuole. J. Biol. Chem. **270:**2525–2534.
33. **Lucero, P., M. Herweijer, and R. Lagunas.** 1993. Catabolite inactivation of the yeast maltose transporter is due to proteolysis. FEBS Lett. **333:**165–168.
34. **Madura, K., and A. Varshavsky.** 1994. Degradation of Gα by the N-end rule pathway. Science **265:**1454–1458.
35. **Matern, H., and H. Holzer.** 1977. Catabolite inactivation of the galactose uptake system in yeast. J. Biol. Chem. **252:**6399–6402.
36. **Medintz, J., H. Jiang, E.-K. Han, W. Cui, and C. A. Michels.** 1996. Characterization of the glucose-induced inactivation of maltose permease in *Saccharomyces cerevisiae*. J. Bacteriol. **178:**2245–2254.
37. **Nehlin, J. O., M. Carlberg, and H. Ronne.** 1989. Yeast galactose permease is related to yeast and mammalian glucose transporters. Gene **85:**313–319.
38. **Nishizawa, K., E. Shimoka, and M. Kasahara.** 1995. Substrate recognition domain of the Gal2 transporter in yeast *Saccharomyces cerevisiae* as revealed by chimeric galactose-glucose transporters. J. Biol. Chem. **270:**2423–2426.
39. **Pringle, J. R., A. E. M. Adams, D. G. Drubin, and B. K. Haarer.** 1991. Immunofluorescence methods for yeast. Methods Enzymol. **194:**565–602.
40. **Ramos, J., K. Szkutnicka, and V. P. Cirillo.** 1989. Characteristics of galactose transport in *Saccharomyces cerevisiae* cells and reconstituted lipid vesicles. J. Bacteriol. **171:**3539–3544.
41. **Rath, S., J. Rohrer, F. Crausaz, and H. Riezman.** 1993. *end3* and *end4*: two mutants defective in receptor-mediated and fluid-phase endocytosis in *Saccharomyces cerevisiae*. J. Cell. Biol. **120:**55–65.
42. **Remaut, E., P. Stanssens, and W. Fiers.** 1981. Plasmid vectors for high-efficiency expression controlled by the p_L promoter of coliphage lambda. Gene **15:**81–93.
43. **Riballo, E., M. Herweijer, D. H. Wolf, and R. Lagunas.** 1995. Catabolite inactivation of the yeast maltose transporter occurs in the vacuole after internalization by endocytosis. J. Bacteriol. **177:**5622–5627.
44. **Richter-Ruoff, B., D. H. Wolf, and M. Hochstrasser.** 1994. Degradation of the *MAT*α2 transcriptional regulator is mediated by the proteasome. FEBS Lett. **354:**50–52.
45. **Riezman, H.** 1993. Yeast endocytosis. Trends Cell Biol. **3:**273–277.
46. **Rohrer, J., H. Benedetti, B. Zanolari, and H. Riezman.** 1993. Identification of a novel sequence mediating regulated endocytosis of the G protein-coupled α-pheromone receptor in yeast. Mol. Biol. Cell **4:**511–521.
47. **Schork, S. M., G. Bee, M. Thumm, and D. H. Wolf.** 1994. Catabolite inactivation of fructose-1,6-bisphosphatase in yeast is mediated by the proteasome. FEBS Lett. **349:**270–274.
48. **Schork, S. M., M. Thumm, and D. H. Wolf.** 1995. Catabolite inactivation of fructose-1,6-bisphosphatase of *Saccharomyces cerevisiae*. Degradation occurs via the ubiquitin pathway. J. Biol. Chem. **270:**26446–26450.
49. **Schwob, E., T. Bohm, M. D. Mendenhall, and K. Nasmyth.** 1994. The B-type cyclin kinase inhibitor $p40^{SIC1}$ controls the G1 to S transition in *S. cerevisiae*. Cell **79:**233–244.
50. **Seufert, W., B. Futcher, and S. Jentsch.** 1995. Role of a ubiquitin-conjugating enzyme in degradation of S and M-phase cyclins. Nature **373:**78–81.
51. **Silve, S., C. Volland, C. Garnier, R. Jund, M. R. Chevallier, and R. Hagenauer-Tsapis.** 1991. Membrane insertion of uracil permease, a polytopic yeast plasma membrane protein. Mol. Cell. Biol. **11:**1114–1124.

52. **Spormann, D. O., J. Heim, and D. H. Wolf.** 1992. Biogenesis of the yeast vacuole (lysosome). The precursor forms of the soluble hydrolase carboxypeptidase yscS are associated with the vacuolar membrane. J. Biol. Chem. **267:**8021–8029.
53. **Szkutnicka, K., J. F. Tschopp, L. Andrews, and V. P. Cirillo.** 1989. Sequence and structure of the yeast galactose transporter. J. Bacteriol. **171:**4486–4493.
54. **Teichert, U., B. Mechler, H. Muller, and D. H. Wolf.** 1989. Lysosomal (vacuolar) proteinases of yeast are essential catalysts for protein degradation, differentiation, and cell survival. J. Biol. Chem. **264:**16037–16045.
55. **Tschopp, J. F., S. D. Emr, C. Field, and R. Schekman.** 1986. *GAL2* codes for a membrane-bound subunit of the galactose permease in *Saccharomyces cerevisiae*. J. Bacteriol. **166:**313–318.
56. **Van den Broek, P. J. A., C. C. M. Van Leeuwen, R. A. Westhuis, E. Postma, J. P. Van Dijken, R. H. Karssils, and R. Ammons.** 1994. Identification of the maltose transport protein of *Saccharomyces cerevisiae*. Biochem. Biophys. Res. Commun. **200:**45–51.
57. **Volland, C., D. Urban-Grimal, G. Geraud, and R. Hagenauer-Tsapis.** 1994. Endocytosis and degradation of the yeast uracil permease under adverse conditions. J. Biol. Chem. **269:**9833–9841.
58. **Wendel, D. L., and L. F. Bisson.** 1993. Physiological characterization of putative high-affinity glucose transport protein of *Saccharomyces cerevisiae* by use of anti-synthetic peptide antibodies. J. Bacteriol. **175:**7689–7996.
59. **Yaglom, J., M. H. K. Linskens, S. Sadis, D. M. Rubin, B. Futcher, and D. Finley.** 1995. $p34^{Cdc28}$-mediated control of Cln3 cyclin degradation. Mol. Cell. Biol. **15:**731–741.